Inverse energy transfer in finite-temperature superfluid vortex reconnections

P. Z. Stasiak, A. Baggaley, and C.F. Barenghi
School of Mathematics, Statistics and Physics, Newcastle University, Newcastle upon Tyne, NE1 7RU, United Kingdom

G. Krstulovic
Université Côte d'Azur, Observatoire de la Côte d'Azur, CNRS,Laboratoire Lagrangre, Boulevard de l'Observatoire CS 34229 - F 06304 NICE Cedex 4, France

L. Galantucci
Istituto per le Applicazioni del Calcolo "M. Picone" IAC CNR, Via dei Taurini 19, 00185 Roma, Italy
(Dated: November 18, 2024)

Lorem ipsum dolor sit amet, consectetuer adipiscing elit. Etiam lobortis facilisis sem. Nullam nec mi et neque pharetra sollicitudin. Praesent imperdiet mi nec ante. Donec ullamcorper, felis non sodales commodo, lectus velit ultrices augue, a dignissim nibh lectus placerat pede. Vivamus nunc nunc, molestie ut, ultricies vel, semper in, velit. Ut porttitor. Praesent in sapien. Lorem ipsum dolor sit amet, consectetuer adipiscing elit. Duis fringilla tristique neque. Sed interdum libero ut metus. Pellentesque placerat. Nam rutrum augue a leo. Morbi sed elit sit amet ante lobortis sollicitudin. Praesent blandit blandit mauris. Praesent lectus tellus, aliquet aliquam, luctus a, egestas a, turpis. Mauris lacinia lorem sit amet ipsum. Nunc quis urna dictum turpis accumsan semper.

Turbulence shapes the physical characteristics of fluid systems, ranging, for instance, from electrically conducting fluids (*magnetohydrodynamics, MHD* turbulence [1]), to classical Newtonian fluids (*Navier-Stokes* turbulence[2]), to superfluid helium and Bose-Einstein Condensates (*quantum* turbulence[3, 4]): turbulence is ubiquitous in the universe, from interstellar media to atomic scales. All turbulent systems are characterised by the existence of a wide range of lengthscales across which inviscid conserved quantities (*e.g.* energy, enstrophy) are transferred without loss, in the spirit of the cascade picture depicted by Richardson [5]. In three-dimensional turbulent flows of classical fluids, turbulence is characterised by a forward cascade – a dissipationless transfer of kinetic energy from large eddies where the energy is injected to increasingly smaller eddies by nonlinear interactions of fluid structures, until viscous dissipation occurs at the smallest length scales [5, 6]. The resulting distribution of energy across length scales follows the celebrated Kolmogorov energy spectrum at the intermediate inertial length scales [2, 6]. Confining classical turbulence to two-dimensions entails fundamentally distinct physics: a dual cascade emerges of both energy and enstrophy (mean squared vorticity) [7, 8], the two conserved quantities in ideal two-dimensional flows. In particular, while we observe a direct cascade of enstrophy, we simultaneously oberve an inverse cascade of energy, *i.e.* an energy transfer towards large scales [9], which may favour the generation and persistence of large scale coherent structures [10].

Remarkably, the same cascade phenomenology is observed in turbulent flows of quantum fluids, *i.e.* fluids whose characteristics are governed by quantum mechanical constraints which kick in at very low temperatures. Examples of such fluids are superfluid helium and Bose-Einstein Condensates (BECs). The dynamics of quantum fluids can be successfully depicted in terms of a two-fluid model [11–13] describing quantum fluids as a mixture of two inseparable fluid components, the superfluid and the thermal component, which interact by means of a mutual friction force [14–16]. The superfluid component is capable of flowing without viscosity and is characterised by vanishing entropy, while its vorticity is entirely confined to effectively one-dimensional structures of atomic core size, the so-called quantum vortices, around which the circulation of the velocity is quantised. The thermal component can be described as a ballistic gas of thermally excited elementary excitations in the context of BECs or as an almost ordinary (classical) viscous fluid in low temperature helium-4. Despite these significant differences with respect to classical fluids, a forward kinetic energy cascade is indeed observed in three-dimensional quantum turbulence in superfluid helium [17–20] and an inverse energy cascade characterises two-dimensional BECs, as shown in theoretical [21–23] and experimental [24, 25] studies.

The idea that the direction of the energy cascade is determined by the dimensionality of the flow and its invariants has been a longstanding belief. However, recent studies have demonstrated that in three-dimensional classical turbulence, the direction of the energy cascade may be controlled by governing the chirality of the flow, *i.e.* the balance between the predominance in the flow of positive or negative helical modes and their interactions. Indeed, by restricting the non-linear energy transfer to homochiral interactions via a suitable decimation of the Navier-Stokes equations,

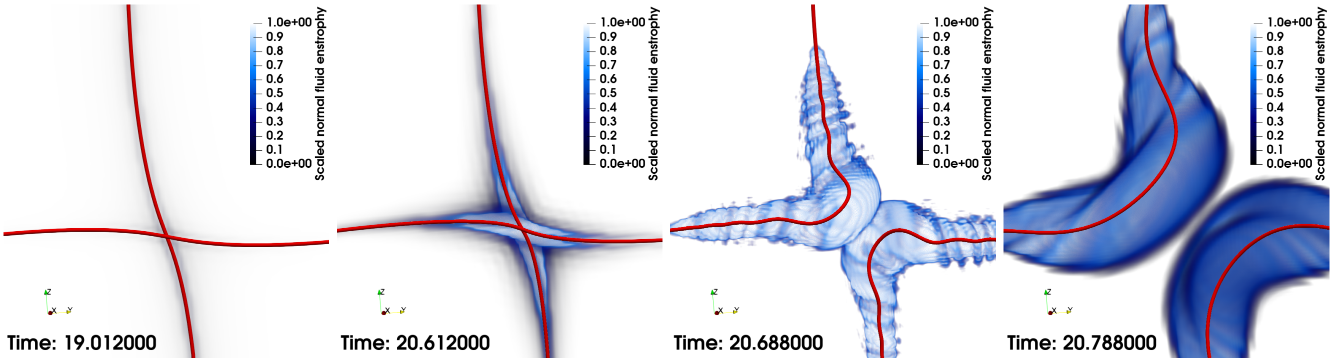

FIG. 1: 3D rendering of an orthogonal vortex configuration, undergoing a vortex reconnection. The red tube represents a superfluid vortex, where the radius has been greatly exaggerated for visual purposes, and the blue volume rendering represents the scaled normal fluid enstrophy $\boldsymbol{\omega}^2/\boldsymbol{\omega}^2_{max}$.

[26, 27], controlling the weight of homochiral interactions [28] or the external injection of positive helical modes at all length scales [29], inverse energy cascades have been observed in three-dimensional turbulence of classical fluids. In brief, when the the flow is synthetically designed to have an enhanced chirality, an inverse energy cascade can observed.

In this work, we unveil a similar dynamics occuring in superfluid helium-4 as a result of a vortex reconnection, an intrinsic event in quantum fluids where two superfluid vortices collide exchanging vortex strands, altering the overall topology of the flow [30–35]. Indeed, we show that the mutual friction force arising from the quantum vortex reconnection is chiral, injecting in the normal fluid prevalently helicity of a given sign. Thus, as a result of a vortex reconnection in superfluids, we observe an increase of the chiral imbalance of the flow, producing a transfer of kinetic energy from small to large scales, similarly to the phenomenology observed in classical flows. Importantly, we stress that this chiral imbalance arises naturally in the normal fluid, *i.e.* as a result of vortex reconnections, ordinary events in superfluids triggered by small-scale quantum pressure dynamics. This is contrast to classical fluid dynamics, where the helical characteristics of the flows producing an inverse energy transfer require a careful synthetic construction [26–29].

In this Letter, to model superfluid helium's dynamics, we employ the recently developed FOUCAULT algorithm [36]. This model parametrises superfluid vortex lines as one-dimensional space curves $\mathbf{s}(\xi, t)$, ξ and t being arclength and time respectively, exploiting the large seperation of length scales between the vortex core, the discretisation of vortex filaments $\Delta\xi$ and the average radius of curvature R_c of vortex lines. Vortices evolve according to the following equation of motion

$$\dot{\mathbf{s}}(\xi,t) = \mathbf{v}_s + \frac{\beta}{1+\beta}\left[\mathbf{v}_{ns}\cdot\mathbf{s}'\right]\mathbf{s}' + \beta\mathbf{s}'\times\mathbf{v}_{ns} + \beta'\mathbf{s}'\times\left[\mathbf{s}'\times\mathbf{v}_{ns}\right], \tag{1}$$

where $\dot{\mathbf{s}} = \partial\mathbf{s}/\partial t$, $\mathbf{s}' = \partial\mathbf{s}/\partial\xi$ is the unit tangent vector, $\mathbf{v}_n$ and $\mathbf{v}_s$ are the normal fluid and superfluid velocities at $\mathbf{s}$, $\mathbf{v}_{ns} = \mathbf{v}_n - \mathbf{v}_s$, and β, β' are temperature and Reynolds number dependent mutual friction coefficients [36].The calculation of the superfluid velocity $\mathbf{v}_s$ is performed via the computation of the Biot-Savart integral de-singularised with standard techniques (see Supplementary Material [37]). The normal fluid is described classically using the incompressible ($\nabla\cdot\mathbf{v}_n = 0$)

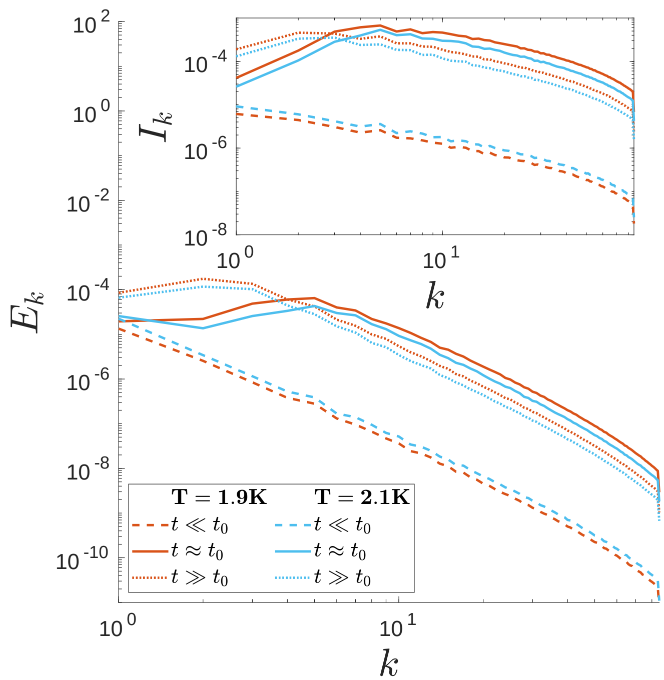

FIG. 2: Normal fluid kinetic energy spectrum $E(k)$ before reconnection (dashed lines), at reconnection (solid lines) and after reconnection (dotted lines) for $T = 1.9K$ and $T = 2.1K$. *Inset:* Energy injection spectrum $I(k)$ arising from the mutual friction forcing at the same snapshots in time.

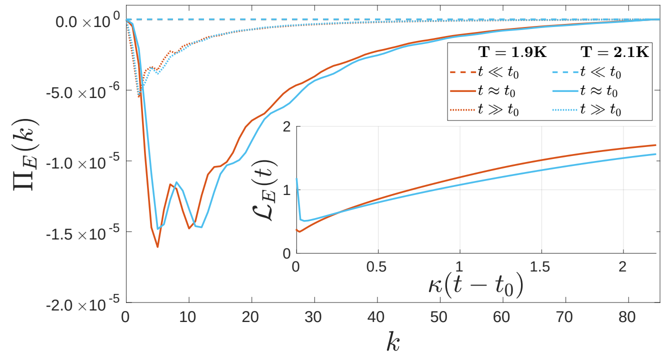

FIG. 3: *Top:* Mutual friction injection spectrum I_k. *Bottom:* Spectral normal fluid kinetic energy flux Π_E. *Inset:* Post reconnection evolution of the integral length scale $\mathcal{L}_E$.

Navier-Stokes equations

$$\frac{\partial \mathbf{v}_n}{\partial t} + (\mathbf{v}_n \cdot \nabla)\mathbf{v}_n = -\frac{1}{\rho}\nabla p + \nu_n \nabla^2 \mathbf{v}_n + \frac{\mathbf{F}_{ns}}{\rho_n} \quad , \qquad (2)$$

where $\mathbf{F}_{ns}$ is the coupling mutual friction force per unit volume, $\rho = \rho_n + \rho_s$, where ρ_n and ρ_s are the normal fluid and superfluid densities, p is the pressure and ν_n is the kinematic viscosity of the normal fluid. We define the mutual friction force $\mathbf{F}_{ns}$ as the line integral of the mutual friction per unit length $\mathbf{f}_{ns}$ [37],

$$\mathbf{F}_{ns}(\mathbf{x}) = \oint_{\mathcal{T}} \delta(\mathbf{x}-\mathbf{s})\mathbf{f}_{ns}(\mathbf{s})d\xi \qquad (3)$$

$\mathcal{T}$ representing the entire vortex geometry. The regularisation of mutual friction is performed using a physically self-consistent scheme [36, 38, 39].

To study the reconnection dynamics, we set two pairs of orthogonal vortices, where corresponding vortices in each pair have oppposite circulation in order to preserve superfluid periodicity along the boundaries, and we consider two distinct temperatures, $T = 1.9K$ and $T = 2.1K$. Vortex pairs are seperated by distance D_ℓ, and each vortex within each pair is seperated by distance d_ℓ, such that $d_\ell \ll D_\ell$. The seperation of scales ensures that the dynamics in the vicinity of the reconnection are dominated by local interactions, and that far-reaching contributions from the other vortex pair are neglible. The evolution of the vortex reconnection of a single pair is reported in Fig. 1.

We first focus the attention on the time evolution of the energy spectrum E, illustrated in Fig. 2, where it emerges clearly that during vortex reconnections, energy is predominantly injected into the normal fluid at intermediate and small length scales: for wavenumbers $|\mathbf{k}| = k > 10$, a significative increase in energy spectral density can be observed in correspondence of reconnection time t_0, namely $E(k, t \approx t_0)/E(k, t \ll t_0) \sim 10^2$. In the post-reconnection regime, we simultaneously observe a small decay of the spectrum at intermediate and small scales ($k > 5$) and its increase at large scales, suggesting a possible mechanism by which energy generated at small length scales is transferred to larger scales. To shed light on this energy spectrum time evolution triggered by reconnections, we analyse the dynamics of the normal fluid flow in terms of the spectral energy budget equation

$$\frac{\partial E(k)}{\partial t} = T(k) - D(k) + I(k) \qquad (4)$$

where $T(k)$ is the spectral kinetic energy transfer function, $D(k) = 2\nu_n k^2 E_k$ is the dissipation spectrum and $I(k)$ is the injection spectrum arising from the mutual friction force $\mathbf{F}_{ns}$. During vortex reconnections, abrupt changes occur in the topology of vortex lines, forming highly curved cusps which immediately relax in structures with small radii of curvature R_c. As $|\mathbf{F}_{ns}| \propto |\dot{\mathbf{s}} - \mathbf{v}_n| \approx |\dot{\mathbf{s}}| \propto 1/R_c$, the resulting scales of energy injection at reconnection are correspondingly much smaller than the large scales, as it can be observed in the inset of Fig. 2. As time evolves, the smallest perturbations on the vortex lines are damped by friction the fastest, resulting in the peak of the injectrum spectrum $I(k)$ to slightly shift towards larger length scales. This shift of the peak of $I(k)$ and its magnitude do not however account for the increase of $E(k)$ observed at the largest scales after reconnection. This increase of energy at the largest scales stems in fact from the energy transfer arising from non linear effects. Indeed, if we compute the energy flux $\Pi(k) = \int_k^\infty T(k')dk'$ (reported in Fig. 3 at different times and temperatures), we observe that $\Pi(k) < 0$ for all k during and after reconnection, with a peak of $|\Pi(k)|$ in the range $5 < k < 15$ when reconnection occurs. This is the evidence of a flux of kinetic energy from small to large scales: *i.e.* vortex reconnections at $T > 0$ trigger an inverse transfer of energy. The effect of kinetic energy transferral to large length scales results in the creation of large scale structures, evident in the evolution of the integral length scale $\mathcal{L}$, where

$$\mathcal{L} = \frac{\pi}{2K}\int_0^\infty \frac{E(k)}{k}dk \qquad (5)$$

and K represents the total turbulent kinetic energy, $K = \int_0^\infty E(k)dk$. In the inset of Fig. 3, $\mathcal{L}$ steadily increases in the post-reconnection region, implying a generation of large scale structure.

In order to explain the observed inverse energy transfer mechanism with a classical argument, we look whether the reconnection process triggers a chirality imbalance. To tackle this issue we use the standard helical decomposition [40] of the incompressible Fourier modes of the normal fluid velocity $\hat{\mathbf{v}}_n(\mathbf{k})$ and of the mutual friction force $\hat{\mathbf{F}}^{\perp}_{ns}(\mathbf{k})$ (the Fourier modes of $\mathbf{F}_{ns}$ parallel to the wavemumber $\mathbf{k}$ do not play any role in the time evolution of $\mathbf{v}_n$ due to the incompressible constraint). According to this helical decomposition, $\hat{\mathbf{v}}_n(\mathbf{k}) = \hat{\mathbf{v}}^+_n(\mathbf{k}) + \hat{\mathbf{v}}^-_n(\mathbf{k}) = v^+_n(\mathbf{k}, t)\mathbf{h}^+(\mathbf{k}) + v^-_n(\mathbf{k}, t)\mathbf{h}^-(\mathbf{k})$, where $\mathbf{h}^{\pm}(\mathbf{k})$ are the two eigenvectors of the curl operator, *i.e.* $i\mathbf{k} \times \mathbf{h}^{\pm}(\mathbf{k}) = \pm k\mathbf{h}^{\pm}(\mathbf{k})$. Accordingly, for the mutual friction force, $\hat{\mathbf{F}}^{\perp}_{ns} = f^+\mathbf{h}^+ + f^-\mathbf{h}^-$. The spectral energy densities corresponding to the helical modes are $E^{\pm}(\mathbf{k}) = (1/2)|v^{\pm}_n(\mathbf{k})|^2$, the total spectral density being $E(\mathbf{k}) = E^+(\mathbf{k}) + E^-(\mathbf{k})$, and the spectral helicity density is $H(\mathbf{k}) = (1/2)\hat{\mathbf{v}}_n(\mathbf{k})\hat{\boldsymbol{\omega}}^*_n(\mathbf{k}) = kE^+(\mathbf{k}) - kE^-(\mathbf{k}) = H^+(\mathbf{k}) - H^-(\mathbf{k})$, where $\boldsymbol{\omega}_n$ is the normal fluid vorticity, '*' indicates the complex conjugate and $H^{\pm}$ is the helicity contribution of each separate helical mode. The rate of change $I^{\pm}(\mathbf{k})$ of the energies $E^{\pm}$ arising from the mutual friction is proportional to the corresponding force helical coefficients $f^{\pm}$, *i.e.* $I^{\pm}(\mathbf{k}) = \mathrm{Re}[f^{\pm}(v^{\pm}_n)^*]/\rho_n$, and the related signed helicity injection is $I^{\pm}_H(\mathbf{k}) = k\mathrm{Re}[f^{\pm}(v^{\pm}_n)^*]/\rho_n$. A chiral imbalance is hence generated if the mutual friction force is helical, *i.e.* if the ratio $|f^+|^2/|f^-|^2 \neq 1$. In Fig. 4, we show the spectra of $|f^+|^2/|f^-|^2$, before, during and after the reconnection event for both working temperatures: it clearly emerges that during and after the reconnection, the mutual friction force is chiral, injecting more positive helicity than negative helicity. As a result, the ratio $\mathcal{H}^+/\mathcal{H}^-$ (reported in the inset of Fig. 4, where $\mathcal{H}^{\pm}(t) = \int H^{\pm}(\mathbf{k}, t)d\mathbf{k}$) increases significantly at reconnection and remains larger than unity even at later times, indicating that the flow is chiral, hence identifying the physical mechanism responsible for the inverse energy transfer observed as a result of the reconnection.

In this Letter, we show that in superfluid helium, in the two-fluid regime ($T \gtrsim 1.5$K), the reconnection of superfluid vortices not only injects punctuated energy in the normal fluid [41], but also triggers in the latter a kinetic energy trasfer towards large scales. This inverse energy transfer arises from the fact that the mutual friction force injecting energy and helicity in the normal fluid is helical due to the development of Kelvin waves on the vortices as a result of the reconnection itself, which is intrinsic event in superfluid dynamics. This helical character of the mutual friction produces a chiral imbalance in the normal fluid which, similarly to what occurs in classical turbulent flows [26, 29], induces a net flux of energy towards the large scales of the flow.

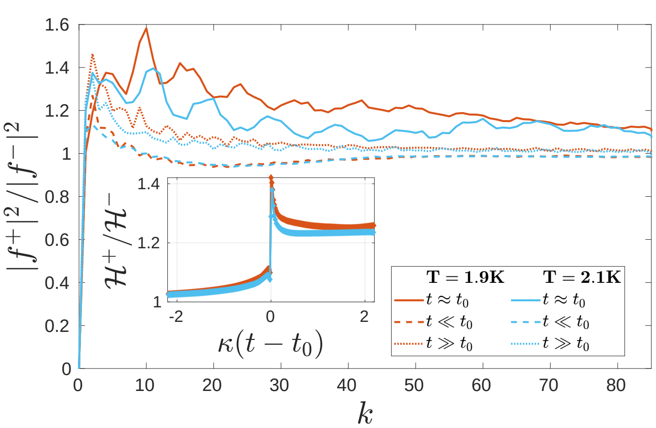

FIG. 4: The ratio of the projected helical mutual friction modes $f^+(k)$ and $f^-(k)$

[1] V. Canuto and J. Christensen-Dalsgaard, Turbulence in astrophysics: Stars, Annual review of fluid mechanics **30**, 167 (1998).

[2] U. Frisch, Turbulence: The Legacy of A. N. Kolmogorov (1995).

[3] CF. Barenghi, HAJ. Middleton-Spencer, L. Galantucci, and NG. Parker, Types of quantum turbulence, AVS Quantum Sci. **5**, 025601 (2023).

[4] C. F. Barenghi, L. Skrbek, and K. R. Sreenivasan, *Quantum Turbulence* (Cambridge University Press, 2023).

[5] L. F. Richardson, *Weather prediction by numerical process* (University Press, 1922).

[6] A. Kolmogorov, The Local Structure of Turbulence in an Incompressible Viscous Fluid for Very Large Reynolds Numbers, Dokl. Akad. Nauk. SSSR **30**, 301 (1941).

[7] R. Kraichnan, Inertial ranges in two-dimensional turbulence, Phys Fluids **10**, 1417 (1967).

[8] G. Boffetta and R. E. Ecke, Two-dimensional turbulence, Annual review of fluid mechanics **44**, 427 (2012).

[9] G. Boffetta and S. Musacchio, Evidence for the double cascade scenario in two-dimensional turbulence, Phys. Rev. E **82**, 016307 (2010).

[10] J. Laurie, G. Boffetta, G. Falkovich, I. Kolokolov, and V. Lebedev, Universal profile of the vortex condensate in two-dimensional turbulence, Phys. Rev. Lett. **113**, 254503 (2014).

[11] L. Tisza, Transport phenomena in helium ii, Nature **141**, 913 (1938).

[12] L. Landau, On the theory of superfluidity, Phys Rev **75**, 884 (1949).

[13] L. Skrbek and K. Sreenivasan, Developed quantum turbulence and its decay, Phys Fluids **24**, 011301 (2012).

[14] B. Jackson, N. Proukakis, C. Barenghi, and E. Zaremba, Finite-temperature vortex dynamics in bose-einstein condensates, Physical Review A—Atomic, Molecular, and Optical Physics **79**, 053615 (2009).

[15] H. Hall and W. Vinen, The rotation of liquid helium ii. i. experiments on the propagation of secound sound in uniformly rotating helium ii, Proc. R. Soc. London A **238**, 204 (1956).

[16] H. Hall and W. Vinen, The rotation of liquid helium ii. ii. the theory of mutual friction in uniformly rotating helium ii, Proc. R. Soc. London A **238**, 215 (1956).

[17] J. Maurer and P. Tabeling, Local investigation of superfluid turbulence, EPL **43**, 29 (1998).

[18] J. Salort, C. Baudet, B. Castaing, B. Chabaud, F. Daviaud, T. Didelot, P. Diribarne, B. Dubrulle, Y. Gagne, F. Gauthier, *et al.*, Turbulent velocity spectra

in superfluid flows, Physics of Fluids **22** (2010).

[19] A. W. Baggaley, L. K. Sherwin, C. F. Barenghi, and Y. A. Sergeev, Thermally and mechanically driven quantum turbulence in helium II, Phys Rev B **86**, 104501 (2012).

[20] L. K. Sherwin-Robson, C. F. Barenghi, and A. W. Baggaley, Local and nonlocal dynamics in superfluid turbulence, Phys. Rev. B **91**, 104517 (2015).

[21] A. S. Bradley and B. P. Anderson, Energy spectra of vortex distributions in two-dimensional quantum turbulence, Physical Review X **2**, 041001 (2012).

[22] M. T. Reeves, T. P. Billam, B. P. Anderson, and A. S. Bradley, Inverse Energy Cascade in Forced Two-Dimensional Quantum Turbulence, Phys. Rev. Lett. **110**, 104501 (2013).

[23] T. Simula, M. J. Davis, and K. Helmerson, Emergence of order from turbulence in an isolated planar superfluid, Phys. Rev. Lett. **113**, 165302 (2014).

[24] S. P. Johnstone, A. J. Groszek, P. T. Starkey, C. J. Billington, T. P. Simula, and K. Helmerson, Evolution of large-scale flow from turbulence in a two-dimensional superfluid, Science **364**, 1267 (2019).

[25] G. Gauthier, M. T. Reeves, X. Yu, A. S. Bradley, M. A. Baker, T. A. Bell, H. Rubinsztein-Dunlop, M. J. Davis, and T. W. Neely, Giant vortex clusters in a two-dimensional quantum fluid, Science **364**, 1264 (2019).

[26] L. Biferale, S. Musacchio, and F. Toschi, Inverse Energy Cascade in Three-Dimensional Isotropic Turbulence, Phys. Rev. Lett. **108**, 164501 (2012).

[27] L. Biferale, S. Musacchio, and F. Toschi, Split energy–helicity cascades in three-dimensional homogeneous and isotropic turbulence, Journal of Fluid Mechanics **730**, 309–327 (2013).

[28] G. Sahoo, A. Alexakis, and L. Biferale, Discontinuous transition from direct to inverse cascade in three-dimensional turbulence, Phys. Rev. Lett. **118**, 164501 (2017).

[29] F. Plunian, A. Teimurazov, R. Stepanov, and M. K. Verma, Inverse cascade of energy in helical turbulence, Journal of Fluid Mechanics **895**, A13 (2020).

[30] J. Koplik and H. Levine, Vortex reconnection in superfluid helium, Phys Rev Lett **71**, 1375 (1993).

[31] G. Bewley, M. Paoletti, K. Sreenivasan, and D. Lathrop, Characterization of reconnecting vortices in superfluid helium, Proc Natl Acad Sci USA **105**, 13707 (2008).

[32] C. Rorai, J. Skipper, R. Kerr, and K. Sreenivasan, Approach and separation of quantum vortices with balanced cores, J Fluid Mech **808**, 641 (2016).

[33] S. Serafini, L. Galantucci, E. Iseni, T. Bienaime, R. Bisset, C. Barenghi, F. Dalfovo, G. Lamporesi, and G. Ferrari, Vortex reconnections and rebounds in trapped atomic bose-einstein condensates, Phys Rev X **7**, 021031 (2017).

[34] L. Galantucci, A. W. Baggaley, N. G. Parker, and C. F. Barenghi, Crossover from interaction to driven regimes in quantum vortex reconnections, Proc Natl Acad Sci USA **116**, 12204 (2019).

[35] A. Villois, D. Proment, and G. Krstulovic, Irreversible dynamics of vortex reconnections in quantum fluids, Physical Review Letters **125**, 164501 (2020).

[36] L. Galantucci, A. W. Baggaley, C. F. Barenghi, and G. Krstulovic, A new self-consistent approach of quantum turbulence in superfluid helium, Eur. Phys. J. Plus **135**, 547 (2020).

[37] See supplementary materials.

[38] P. Gualtieri, F. Picano, G. Sardina, and C. M. Casciola, Exact regularized point particle method for multiphase flows in the two-way coupling regime, Journal of Fluid Mechanics **773**, 520 (2015).

[39] P. Gualtieri, F. Battista, and C. M. Casciola, Turbulence modulation in heavy-loaded suspensions of tiny particles, Physical Review Fluids **2**, 034304 (2017).

[40] F. Waleffe, The nature of triad interactions in homogeneous turbulence, Phys Fluids A **4**, 350 (1992).

[41] P. Stasiak, Y. Xing, Y. Alihosseini, C. Barenghi, A. Baggaley, W. Guo, L. Galantucci, and K. G, Quantum vortex reconnections, arXiv , 2411.08942 (2024).